REMOTE SENSING OF MICROMETEOROLOGICAL QUANTITIES

By

R. L. Coulter
Environmental Research Division
Argonne National Laboratory
Argonne, IL 60439-4843

Paper for

11th International Symposium on Acoustic Remote sensing of the atmosphere and Oceans

24-28 June 2002, Rome, Italy

Work at Argonne National Laboratory was supported by the U.S. Department of Energy, Office of Science, Office of Biological and Environmental Research, Environmental Sciences Division, under contract W-31-109-Eng-38.

The submitted manuscript has been created by the University of Chicago as Operator of Argonne National Laboratory ("Argonne") under Contract No. W-31-109-ENG-38 with the U.S. Department of Energy. The U.S. Government retains for itself, and others acting on its behalf, a paid-up, nonexclusive, irrevocable worldwide license in said article to reproduce, prepare derivative works, distribute copies to the public, and perform publicly and display publicly, by or on behalf of the Government.

REMOTE SENSING OF MICROMETEOROLOGICAL QUANTITIES

R. L. Coulter

Argonne National Laboratory

Argonne, IL 60439 USA

[rlcoulter@anl.gov]

Abstract

This overview of the uses of sodars in meteorological applications categorizes the applications by signal source, specifically amplitude, frequency, or "visualization" for example, of vertical time sections of signal amplitude. Examples are shown of data derived from each category. A final section presents the potential for using groups of sodars in networks with other instruments to estimate quantities such as divergence.

1. INTRODUCTION

The use of acoustic remote sensing in meteorology has become well known over the three plus decades since practical applicaions began with McAllistar (1969). Because of the slow (relative to its electromagnetic cousins, the lidar and radar) propagation speed acoustic sensing is well suited to micrometeorological applications focused close to the earth's surface. In addition, because of its relatively simple design and (potentially) small cost, acoustic remote sensing is available to a variety of institutions, and the results of data analysis can be useful in many different situations. There are, however limits to its usefulness due to a variety of sources, including noise contamination, atmospheric absorption, bandwidth limitations, and volume averaging effects, that are important considerations in sound detection and ranging (sodar) applications.

Three primary types of information are available from conventional sodar that are directly useful in micrometeorological applications:

(1) Signal amplitude is proportional to the temperature and velocity structure parameters (Tatarskii, 1961; Brown, 1972, for example) and so can be related to atmospheric temperature variance (and then to heat flux) and velocity variance (and then to mechanical turbulence and dissipation rate). Signal amplitude cannot, however, be used to measure the temperature gradient or temperature profile directly, both because the source of the acoustic scattering is turbulent fluctuations in the temperature field on the order of the wavelength of the sound (Kallistratrova, 1961). Scattering from the mean temperature gradient structure is too small to be detected, except possibly in some rare instances (Balsley, personal communication).

(2) Frequency of the signal amplitude or, more appropriately, the Doppler shift of the signal is proportional to the speed of the scattering source (turbulent fluctuations) relative to the wave front of the acoustic signal, most often along the direction of the incident signal (in monostatic operation) which can be related to the atmospheric wind speed (Hall, 1972, for example if the turbulent fluctuations are "scalar" and move with the mean wind.

(3) The spatial and temporal structure of the signal, an amorphous quality is sometimes defined with objective routines that analyze the time and height variations in (1) and (2) above, such as mixed layer height, z_i, but it is most often derived by visual interpretation of vertical time sections of signal amplitude; the resultant "measurements" are often amorphous, as well, relating more to conditions than quantities, such as "convective", "stable", "stratified", and "waves." Although these qualities may not be directly usable in computations, they often impart more information than a long series of computations.

This paper discusses the derived quantities from each of these information sources that are useful in mesoscale atmospheric measurements; however, it is organized by meteorological quantity (profiles, fluxes, heights). Nest we give a few examples of the use of sodars in networks and in conjunction with radar wind

profilers to extend their usefulness in measuring, for example, divergence. Acknowledging the large number of contributors to this field adequately is impossible ane the selected references are representative rather than comprehensive.

2. METEOROLOGICAL PROFILES

Measurement of the atmospheric wind speed as a function of height is perhaps the most common use of the sodar. The sodar generally uses a three-beam, monostatic configuration to obtain three components of motion in three orthogonal planes from Doppler shifts of the scattered acoustic signal, from which the horizontal wind speed, horizontal wind direction and vertical wind speed can be determined as a function of height (Hall, 1972; Mastrantonio and Fiocco, 1982). With conventional sodar (frequency between 1 kHz and 2 kHz) the maximum range is normally near 1 km, although larger heights have been achieved with good signal sources (significant temperature and wind structure at large heights), long-duration transmision pulses, and low signal frequency (reducing the effects of atmospheric absorption). In dry conditions with relative humidity near 20%, atmospheric absorption severely limits the maximum height (Coulter, 1990) attainable with these systems. The minimum usable range of such a system is normally 20-40 m, depending on pulse length and the site and orientation of the antenna.

The development of the minisodar (Moulsley et al., 1981; Weill et al., 1986; Coulter and Martin, 1986) maximizes the information near the surface by using high frequencies (near 4500 Hz) and short pulse durations (see Table 1). As a result minisodars normally have usable data near 10 m above the surface, although some systems have been used within 2 m of the surface (Asimakopolous et al., 1983); however, the maximum attainable height of these systems is normally 200 m or less. Because they use higher frequencies than conventional sodars, the Doppler sensitivity,

$$S_d = 2f/c\,, \qquad (1)$$

where f = transmit frequency, and c = speed of sound, is 2 to 4 times larger for minisodars. This sensitivity can result in higher-accuracy wind estimates. In addition, such systems normally use shorter pulse lengths to achieve better vertical resolution, an important consideration near the surface. Combining the minisodar with conventional sodar or radar wind profiler yields a fairly complete picture of the atmosphere between 10 m and 10 km.

Table 1. Comparison of typical conventional sodar and minisodar

Quantity	Conventional sodar	Mini sodar
Frequency	1–2 kHz	4 kHz – 6 kHz
Scattering element size	8–17 cm	3 cm – 4 cm
Range	40 m–1 km	5 m – 200 m
Range gate	20 m	5 m
Doppler sensitivity	6–12 Hz/(m/s)	24–36 Hz/(m/s)
Strength	z_i, wind profile	Turbulence, sfc layer
Weakness	σ_w, sfc layer	z_i
Size	2 m X 2 m X 3 m	1 m X 1 m X 1 m

A further application of minisodars becomes evident during precipitation. Because of their relatively large Doppler sensitivity, minisodars can often simultaneously determine the scattering from raindrops and that from the atmosphere; the Doppler spectra for the scattering from rain can then be used to estimate the droplet size distribution, as well as the rain rate (e.g., Coulter, 1990 or Bradley, 1996).

The profile of the standard deviation of vertical velocity, σ_w, is often used as a measure of atmospheric stability with sodar data. Gaynor (1994) showed good agreement between conventional sodars and tower-mounted sonic anemometers during daytime, when fluctuations in w are large. During nighttime, however, the contributions to the variance in the signal from the measurement system itself (Spizzichino, 1974; Neff and Coulter, 1986) can become a lower limit (near 0.25 m/s) to these measurements. Better results have been achieved with minisodars (Coulter and Martin, 1986; Weill et al., 1986; Asimakopoulos et al., 1983) (Fig. 1). Nevertheless, compensation for an appropriate estimate of system contributions to the variance must be included. In principle, the standard deviation of the horizontal components of motion can also be derived; however the difficulty of measuring these values is compounded because they are derived from data from multiple directions (at least one tilted beam plus the vertical beam, for example). The time delay between measurements of these signals adds considerable complexity to the determination of the true system variance (Kristensen and Gaynor, 1986).

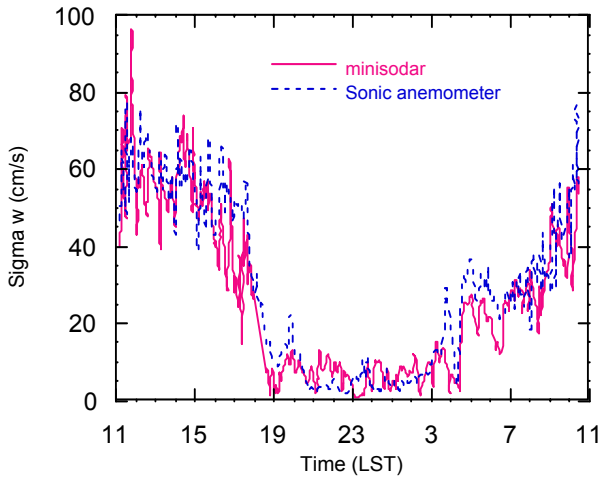

Figure 1. Time series of σ_w from a high-frequency minisodar and nearby sonic anemometer at a height of 23.5 m.

.

Profiles of C_T^2 can be obtained from the range gated signal return power, P, if the system is calibrated, either by comparing signal levels with local measurements of C_T^2 from a tower, for example or by calibrating the system sensitivity with collocated pressure transducers (Coulter, 1979b) and calculating C_T^2 from the coupled equations (Thomson et al., 1978; Clifford, 1972)

$$P(\theta,r) = P_0 (A_{rec}/r^2)\left(A_c L_v / A_t\right)\sigma(\theta,r)$$

$$\exp\left[-\int_T^r \alpha(r)dr\right]\exp\left[-\int_r^R \alpha(r)dr\right], \qquad (2)$$

$$\sigma(\theta,r) = \frac{0.03k^{1/3}\cos^2(\theta)}{\sin(\theta/2)^{-11/3}}$$

$$\left[\left(\frac{C_v^2(r)}{c^2}\right)\cos^2(\theta/2) + 0.13\left(\frac{C_T^2(r)}{T^2}\right)\right], \qquad (3)$$

where P_0 is the transmitted power, A_{rec} is the area of the receiver, L_v is the length of the instantaneous scattering volume, A_c is the scattering area common to the transmitter and receiver beams, A_t is the area subtended by the transmit beam at the scattering location, □ is the scattering angle, □ is the atmospheric attenuation, □ is the scattering cross section, k is the wave number, C_v^2 is the velocity structure parameter, c is the speed of sound in air, r is the distance to the scattering volume, and inertial subrange, isotropic turbulence is assumed (Brown, 1978). In the most commonly used, monostatic, configuration θ = 180 deg, and $A_c = A_r$.

The height dependence of C_T^2 is a very useful tool in determining atmospheric stability. In the convective boundary layer (unstable conditions), a –4/3 power dependence on z is well established theoretically (Wyngaard et al., 1971) and experimentally (Neff, 1975). At the top of the mixed layer values of C_T^2 increase because of turbulent mixing from thermals within the mixed layer that penetrate into the stratified air above; thus the increase in C_T^2 above a well-defined –4/3 logarithmic dependence on z provides a measure of z_i as well as the convective nature of the boundary layer during daytime (Fig. 2).

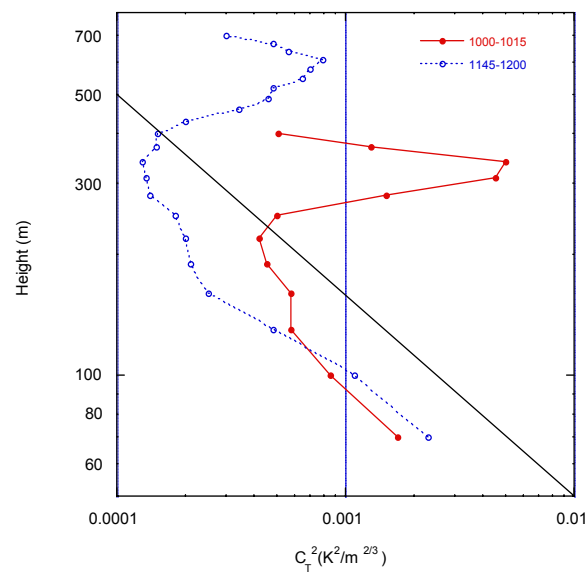

Figure 2. Example of typical profiles of C_T^2 obtained above the Konza Prairie on June 27, 1987, that illustrates the deepening mixed layer from 300 m at 1000 hr to 650 m at 1145 with a convective mixed layer below.

Values of C_v^2 can be determined from (3) as well, if a second measure of P(z) is available from a second receiver located at some angle other than 180 deg or 90 deg (Hall, 1972; Coulter and Underwood, 1980). This measurement is difficult to perform accurately because of the complicated nature of the scattering volume and refraction effects. This parameter can also be determined from its definition,

$$C_v^2 = \left\langle \left(\frac{v(r) - v(r+dr)}{r^{1/3}} \right)^2 \right\rangle, \qquad (4)$$

where v is the component of wind velocity, dr is the separation along the direction of the velocity, and the brackets indicate an ensemble average, so long as the separation distance between measured values is within

the dissipation range of the turbulence spectrum and the system variance contributions and volume averaging effects (Gaynor, 1977; Kristensen, 1978; Coulter, 1990) are taken into account. The estimate of C_v^2 and C_T^2 permits a large number of turbulence parameters to be estimated such as turbulence dissipation rate, $\varepsilon = 0.36\left(C_v^2\right)^{3/2}$ and temperature variance dissipation rate, $N = 0.31 C_T^2 \varepsilon^{1/3}$ (Brown and Hall, 1978). Figure 3 shows such a calculation obtained using minisodar data from within the nocturnal boundary layer (NBL), during an episode of turbulence. In this case C_v^2 was computed from vertical velocity differences rater than signal amplitudes. The NBL is a region particularly suitable to investigation with minisodars because of its limited extent and highly irregular behavior.

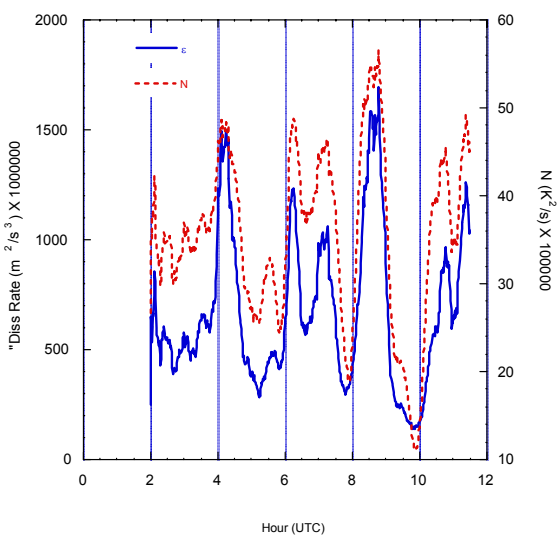

Figure 3. Time series of dissipation rate and temperature variance destruction rate derived from instantaneous velocity estimates 20 m above the ground obtained with a minisodar. Note the periodic, sudden increases associated with breaking waves in the NBL.

FLUXES

One of the most important parameters in the definition of the surface and well-mixed layer of the atmosphere is the surface heat flux, H. In unstable conditions during daytime, the sodar provides an attractive means for estimating this value. Wyngaard et al.(1971) showed that in convectively unstable conditions,

$$H = 0.48\rho c_p (g/T)^{1/2}\left(C_T^2\right)^{4/3}, \qquad (5)$$

where ρ is atmospheric density, c_p is the specific heat of air at constant pressure, and g is the acceleration of gravity. Observationally, C_T^2 has been found to follow a –4/3 dependence well above the surface layer (Fig. 3). Thus, for a profile of C_T^2 that follows a –4/3 power dependence on z, H can be estimated from (5).

Several investigators have used this approach successfully to estimate H with sodar data (Neff. 1975 Weill, et al., 1980; Coulter and Wesely, 1980). Coulter and Wesely (1980) noted that the relationship needs to be modified, when the Bowen ratio (β = H/LE, where LE = latent heat) is less than 0.3, by the factor,

$$\left[1 + \left(0.07/\beta_s\right)^2\right]^{-1} \qquad (6)$$

to account for moisture effects. Measurements with this approach are generally more variable than those with sonic anemometers, for example, principally because the measurement of C_T^2 is not much more accurate than 3 dB. A critical parameter in this approach is the correction for atmospheric absorption, which can be quite large at higher frequencies; thus, application of this approach can be more difficult for minisodars than with conventional devices.

A second, sometimes easier and perhaps more robust approach to this parameter was introduced by Weill et al., (1980) who showed that the profile of σ_w^3 can be calculated and also that in convective conditions the local heat flux H_l at height z can be calculated as

$$H_l = 0.60\rho c_p (\Theta/g)\left(\frac{\sigma_w^3}{z}\right), \qquad (7)$$

where Θ is the potential temperature. This vaue can then be extrapolated into the surface layer to estimate H. Contributions to σ_w from mechanical turbulence near the surface contribute to nonlinearity of the relationship in this region. As always, as higher moment products are calculated, error contributions mount.

The momentum flux, $\rho c_p u_*$, can also be estimated directly with sodars, within some necessary assumptions. From the instantaneous (unaveraged) measures of w and the along-wind and cross-wind components of the horizontal wind, u and v, we can measure u_* directly as

$$u_* = \left[(u'w')^2 + (v'w')^2\right]^{1/4}, \qquad (8)$$
$$u' = u - ubar$$
$$v' = v - vbar,$$

where ubar and vbar are the mean values of the wind components. Weill et al. (1988) and Kalogiros et al. (1999) employd this method; Beyrich and Kotroni

(1993) used it to incorporate u* into an estimate of nocturnal boundary layer height. When this calculation is done with data from tower-mounted sonic anemometers, care must be taken that the upwind fetch is much larger than the measurement height; the same requirements are required for the sodar estimates, but they are more difficult to achieve because sodar measurements are usually considerably higher than those of a sonic anemometer. It is also important, once again, to consider carefully all the contributions to the products of fluctuating quantities due to the derivation of estimates of u' and v' from multiple beams located at different points in space and time (Kristensen, 1978).

3. VISUALIZATION

The vertical time section, a gray- or color-scale display of signal amplitude plotted versus time and height (Fig. 4) is in some ways the most useful display of sodar data.)ne picture, can show the diurnal variation of the atmospheric boundary layer (Neff and Coulter, 1986). For example, the time variation of z_i discussed above can be defined at a number of time scales. A considerable body of discussion has addressed this topic (Beyrich, 1997a; Beyrich et al., 1998; Coulter, 1979b, for example). To date no automated, objective routine can perform as well as the human mind at defining this layer. The onset of convective conditions is evidensed in Fig. 4a by the classic "grass-like" structures at 1500 UTC, somewhat after the mixed layer has begun to rise. The depth of the NBL is clearly evident beginning at 1800 hr, with a quasi-linear rise rate (or more appropriately depth increase). In this case the remains of the previous daytime's capping inversion is still evident; hence the transition layer is known to lie between the top of the NBL and the remains of the previous days capping inversion. The character and evolution of "elevated stable layers" (ESLs) within and above the transition region are evident as well (Helmis et al., 2000). A simple graphical interface that defines the heights of layers of interest (z_i, NBL, etc.) by cursor movements can quickly and accurately define regions of interest for more quantitative investigation. The importance of measurements of z_i is particularly evident over urban areas where the mixed layer is normally higher during daytime and less stable during nighttime than in the surrounding environs Argentini et al. (1999) and Pekour and Kallistratova (1993) have reported good examples of urban studies with sodar.

When the time scale is expanded, the vertical time section provides further evidence of atmospheric structure (Fig. 4b). Wave motion and patchy turbulence are evidence of the complicated nocturnal structure of the NBL. However, defining at least a component of the wavelength and the vertical extent of the wave motion is straightforward.

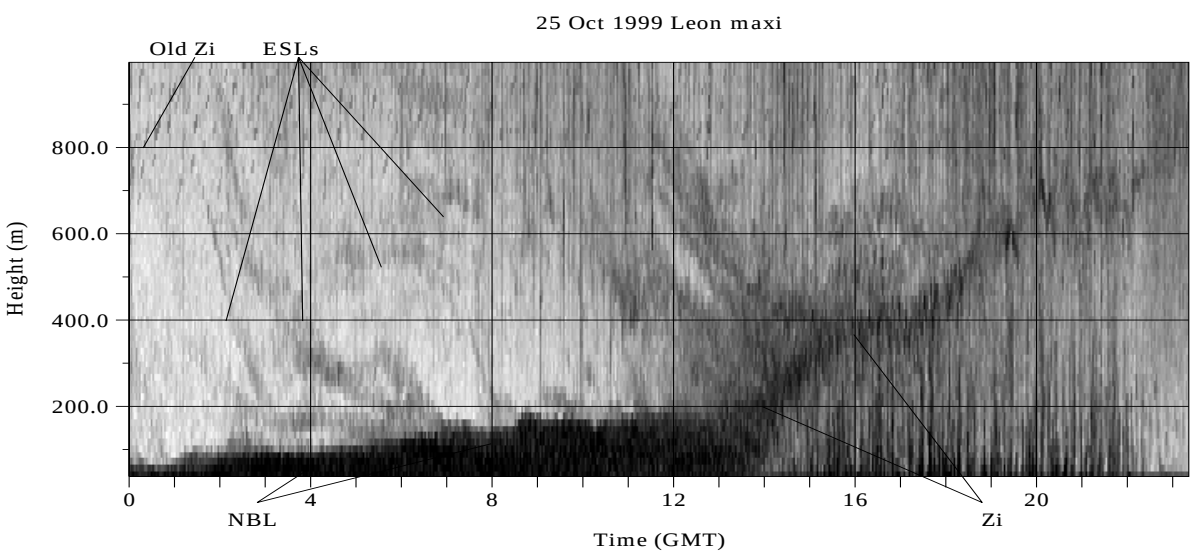

Figure 4a. An example of a vertical time section for a 24-hr period over the Amospheric Boundary Layer Experiments area in Kansas during the 1999 Cooperative Atmosphere-Surface Excange Study with some of the boundary layer parameters indicated.

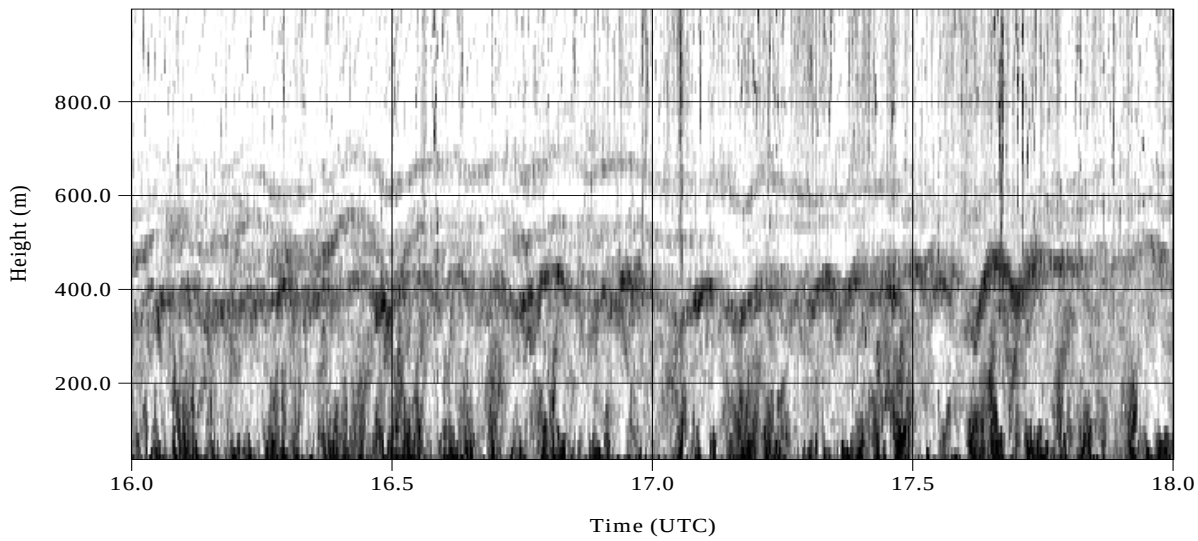

Figure 4b. Enlargement of a 2-hr period from Fig. 4a showing well defined wave motion at and above the capping inversion during daytime.

4. NETWORKS

Increasingly scientists are coming to realize that it is often necessary to combine results from several instruments to fully define a problem. Examples are the Lindenburg Column (Beyrich et al., 1997b) and the Atmospheric Boundary Layer Experiments (ABLE) facility. There the high-resolution capabilities of the sodar or minisodar near the earth's surface are combined with the coarser time and space resolution but considerably larger range of the radar wind profiler. As field studies and continuous time series cover larger horizontal extents, it is important to measure vertical profiles at locations separated horizontally but still "connected" meteorologically. Calculation of horizontal divergence with such systems enables the potential estimation of large-scale vertical velocities that are not directly measurable with remote sensing systems. Using the divergence theorem, we can calculate the divergence at a given height, D_z,

$$D = \oint(udy - vdx) \Big/ 0.5\oint(xdy - ydx) \quad , \qquad (9)$$

where the integral is counterclockwise over the measurement locations, by summing over pairs of stations around the perimeter as shown by Boers, et al. (1976). Then the vertical velocity associated with the divergence is

$$w_{div} = -\sum_z D_z \Delta z \, , \qquad (10)$$

where Δ_z is the appropriate range gate. We have implemented this calculation with the three minisodar-radar wind profilers at the ABLE facility (Coulter, 1999) and have used it to obtain values of w_{div}, which should increase linearly with height if the divergence used in (10) is constant with height. Figure 5 shows the variation of this value 500 m above the surface with time during the 1999 Cooperative Atmosphere-Surface Exchange Study that took place at the ABLE site in Kansas, USA, during October 1999. The correlation of significant positive w_{div} with frontal passages and negative w_{div} with clear, steady conditions is an encouraging demonstration of the use of multiple systems in micrometeorological applications. A significant problem with this type of calculation lies in the interpretation of the data from multiple sites at different elevations. A terrain-following coordinate system might be appropriate for stable conditions with relatively small separations. However, in unstable conditions a geopotential coordinate system would seem a likely candidate. For the data displayed in Fig. 5, the level for each computation of the divergence changes gradually from a terrain-following system to a geopotential coordinate system, with a height above the highest location equal to the maximum height difference between measurement locations.

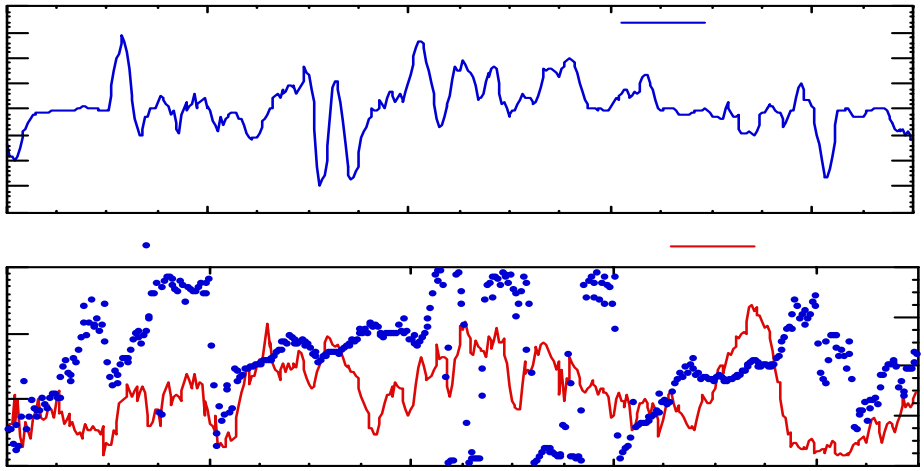

Figure 5. Ten-day time series of vertical motion calculated from the divergence of horizontal winds at the ABLE site in Kansas, USA. Note the relatively large values (approximately 3 cm/s) during frontal passages (wind direction change from south to north) and strong subsidence during conditions with little wind direction change. Each value represents a 30-min average smoothed with a seven-point running mean.

5. CONCLUSION

Sodar continues to provide the ability to characterize the atmospheric boundary layer to degrees under-used by much of the scientific community. The continued interest of atmospheric scientists in answering basic questions required by society is needed to realize fully the beneficial use of sodars.

6. ACKNOWLEDGMENT

Work supported by the U. S. Department of Energy, Office of Science, Office of Biological and Environmental Research, under contract W-31-109-Eng-38.

6. REFERENCES

Argentini, S., G. Mastrantonio, and F. Lena, 1999: Case studies of the wintertime boundary-layer Structure in the urban area of Milan, Italy, *Bounary Laer Meteorol*. **93**, 253-267.

Asimakopolous, D. N., R. S. Cole, S. J. Caughey, and B. A. Crease, 1976: A quantitative comparison between acoustic sounder returns and the direct measurement of atmospheric temperature fluctuations. *Boundary Layer Meteorol*. **10**, 137-148.

Asimakopolous, T. J. Mousley, C. G. Helmis, D. P. Lalas, and J. Gaynor, 1983: Quantitative low-level acoustic sounding and comparison with direct measurements. *Boundary Layer Meteorol*. **27**, 1-26.

Beyrich, F., and V. Kotroni, 1993: Estimation of surface stress over a forest from sodar measurements and its use to parameterize the stable boundary layer height, *Boundary Layer Turbul.* **66**, 93-106.

Beyrich, F., 1997a: Mixing height estimation from sodar data - A critical discussion. *Atmos. Environ.* **31**, 3941-3953.

Beyrich, F., D. Engelbart, U. Goersdorf, J. Neisser, and U. Weisensee, 1997b: Towards the "Lindenberg column" - simultaneous measurements of vertical profiling systems. *Extended Abstr. of Cost-76 Profiler Workshop 1997*, Engelberg, Switzerland **1**, 166-169.

Beyrich, F. D., and S. E. Gryning, 1998: Estimation of the entrainment zone depth in a shallow convective boundary layer from sodar data, *J. Appl. Meteorol*. **37**, 255-268.

Boers, R., E. W. Eloranta, and R. L. Coulter, 1984: Lidar observations of mixed layer dynamics: Tests of parameterized entrainment models of mixed layer growth rate. Journ. Appl. Meteorol., **23**, 247-266.

Bradley, S., 1996: A high frequency Doppler acoustic precipitation radar. *Proceedings of the Eighth International Symposium on Acoustic Remote Sensing of the Atmosphere and Oceans*, , A. M. Obukhov Institute of Atmospheric Physics, Moscow, Russia, pp 3.13-3.18.

Brown, E. H., 1972: Acoustic-Doppler-radar scattering equation and general solution. *J. Acoust. Soc. Am*. **52**, 1391-1396.

Brown, E. H. 1978: Quantitative acoustic measurements of atmospheric turbulence. *Preprints 4th Symposium on meteorological observations and instrumentation*, April 10-14, Denver, Colorado. pp. 275-278.

Brown, E. H. and F. F. Hall, 1978: Advances in Atmospheric Acoustics. *Rev. Geophys. and Space Physics.* **16**(1), pp 47-109.

Clifford,S. F., 1972: "Propagation and Scattering in a random Media". Remote Sensing of the Troposphere, American Meteorological. Society, Boston, Massachusettes. 11-1 through 16-24.

Coulter, R. L. 1979a: Sodar Calibration Results. *Argonne National Laboratory, Radiological and Environmental Division, Annual Report* ANL-78-65, Pt. IV, pp. 14-18.

Coulter, R. L., 1979b. A comparison of three methods for measuring mixing-layer height. *J. Appl. Meteorol*. 18, 1495-1499.

Coulter, R. L., and M. L. Wesely, 1980: Estimates of surface heat flux from sodar and laser scintillation measurements in the unstable boundary layer. *J. Appl. Meteorol*. **19**, 1209-1222.

Coulter, R. L., and K. H. Underwood, 1980: Some turbulence and diffusion parameter estimates within cooling tower plumes derived from sodar data. *J. Appl. Meteorol.* **19**, 1395-1404.

Coulter, R. L., and T. J. Martin, 1986: Results from a high power, high frequency sodar, *Atmos. Res.* **20** # 2-4, 257-270.

Coulter, R. L., T. J. Martin, and T. Weckwerth, 1989: Minisodar measurements of rain. *J. Oceanic and Atmos. Technol*. **6**, 369-377.

Coulter, R. L., 1990: A case study of turbulence in the stable nocturnal boundary layer. *Boundary. Layer Meteorol*. **52**, 75-91.

Coulter, R. L., 1997: Turbulence variables derived from sodar data In: Acoustic Remote Sensing Applications, Chapter 9, ed. Dr. S. P. Singal,

Narosa Publishing House, Delhi, India, pp. 191-202.

Coulter, R. L., 1999: Convergence estimates over the ABLE region during CASES-97 obtained from radar wind profiler and sodar data. *Proceedings of 13th Conference on Boundary Layers and Turbulence,* Jan. 10-15, Dallas, Texas, American Meteorol. Soc., , pp 508-511

Gaynor, J. E., 1977: Acoustic dDoppler measurements of atmospheric boundary layer velocity structure functions and energy dissipation rates. *J. Appl. Meteorol*. **16**, 148-155.

Gaynor, J. E., 1994: Accuracy of sodar wind variance measurements, *Int. J. Remote Sensing* **15**, 313-324.

Hall, F. F. 1972: "Temperature and wind structure Studies by acoustic echo-sounding". *Remote Sensing of the Troposphere*, American Meteorological Society, Boston, Massachusettes, 18-1 through 18-23.

Helmis, C. G., J. A. Kalogiros, and D. N. Asimakopoulos, 2000: Estimation of potential-temperature gradient in turbulent stable layers using acoustic sounder measurements, *Quart. J. Royal. Meteorol. Soc.* **126 (**562**)** 31-61.

Kallistratova, M. A., 1961: Experimental investigation of sound wave scattering in the atmosphere. Tr. Inst. Fiz. Atmos., *Atmos. Turbulentmost*, **4**, 203-256. (English translation, U. S. Air Force FTD TT-63-441)

Kalogiros, J. A., C. G. Helmis, K. H. Papadopoulos, 1999: Estimation of ABL parameters using the vertical velocity measurements of an acoustic sounder, *Boundary. Layer Meteorol*. **91** 412-449

Kristensen, L., 1978: *On sodar techniques*. Riso National Laboratory, Riso Report 381, August.

Kristensen, L., and Gaynor, J, 1986: Errors in second moments estimated from monostatic Doppler sodar winds, Part I: Theoretical Description. *J. Atmos. Oceanic Technol*. **3**, 523-528.

Little, C. G., 1969: Acoustic methods for the remote probing of the lower atmosphere. *Proceed. I.E.E.E*. **57**, 571-578.

Mastrantonio, G., and G. Fiocco, 1982: Accuracy of wind velocity determination with Doppler sodars. *J. Appl. Meteorol*., **21(**6**)**: 823-830.

Moulsley, T. J., D. N. Asimakopoulos, R. S. Cole, B. A. Crease and S. J. Caughey: 1981: Measurement of boundary layer structure parameter profiles by acoustic sounding and comparison with direct measurements. *Quart. Jroyal Meteorol. Soc.* **107**, 203-230.

Neff, W. D., 1975: *Quantitative evaluation of acoustic echoes from the planetary boundary layer*. ERL 322-WPL 38, National Oceanic and Atmospheric Administration, Boulder, Colorado.

Neff, W. D., and R. L. Coulter, 1986: Acoustic remote sensing, *Probing the Atmospheric Boundary Layer,* American Meteorological. Society, Boston, Massachusettes pp.. 201 - 235.

Pekour, M. S., and M. A. Kallistratova, 1993: Sodar study of the boundary layer over Moscow for air-pollution application. *Appl. Phys. B.,* **57**, 49-55.

Spizichino, A. 1974: Discussion of the operating conditions of a Doppler sodar. *J. Geophys. Res*. **79**, 5585-5591.

Tatarskii, V. I., 1961: *Wave Propagation in a Turbulent Medium*. Translated from Russian by R. A. Silverman, Dover, New York.

Thomson, D. W., R. L. Coulter, and Z. Warhaft, 1978: Simultaneous measurements of turbulence in the lower atmosphere using sodar and aircraft. *J. Appl. Meteorol*. **17**, 723-734.

Weill, A., C. Klapisz, B. Strauss, F. Baudin, C. Jaupart, P. VanGrundebeeck, and J. P. Goutorbe, 1980: Measuring heat flux and structure function of temperature fluctuations with an acoustic Doppler sodar. *J. Appl. Meteorol*. **19**, 199-205.

Weill, A., 1983: Atmospheric applications of sodar *Proceedings of the second International Symposium on Acoustic Remote sensing of the*

Atmosphere and Oceans, Rome, Italy, Aug. 29 - Sept. 1, pp. I-1 through I-41.

Weill, A., C. Klapisz, and F. Baudin, 1986: The CRPE minisodar: Applications in micrometeorology and in physics of precipitations. *Atmos. Res*. **20**, 317-335.

Weill, A., C. Mazaudier, F. Leca, and M. Masmoudi, 1988: Doppler sodar and fluxes measurement. *Proc. 4th ISARS 1988*, Canberra, Australia, 30, 1-6.

Wyngaard, J. C., J. Izumi, and S. A. Collins, Jr, 1971: Behavior of the refractive index structure parameter near the ground. *J. Opt. Soc. Am*. **61**, 1646-1650.